Experimental Studies of Propeller Induced Flow over a Typical Micro Air Vehicle

S.Sudhakar[1], Chandan Kumar[2] and L.Venkatakrishnan[3]
CSIR, National Aerospace Laboratories, Bangalore, India ,560017

An experimental study has been carried out to explore the effect of propeller induced slipstream on the flow field of a fixed wing micro air vehicle (MAV). Tests were conducted at freestream velocity of 10m/s, corresponding to Reynolds number based on root chord of about 160000. Flow pattern on the surface of MAV planform with propeller-on and off condition was captured using oil flow visualization at four angles of incidence. Mean flow field on the MAV planform at four chordwise planes with propeller-on and off condition were measured using stereo PIV technique at angle of incidence of 24°. Little difference has been seen on the oil flow pattern at 10° and 15° angle of incidence between propeller-off and on condition. Small asymmetry in the flow topology was observe at 20° angle of incednce. Significant difference in flow field was observed at 24° between propeller-on and off condition. The induced slipstream from the propeller makes the flow well attached over the wing planform.

Nomenclature

X	=	streamwise coordinate
Y	=	vertical coordinate
Z	=	transverse coordinate
U_∞	=	freestream velocity
U	=	streamwise velocity
V	=	vertical velocity
W	=	tangential velocity
c	=	chord
AR	=	aspecratio

I. Introduction

The design and development of Micro Air Vehicles (MAVs) has become an important field in the aerospace community for its numerous military and civilian applications like surveillance, search and rescue, damage assessment and reconnaissance. Most of the MAVs have low aspect ratio (AR≈1.0-1.5) planforms with span between 15-30cm, forward velocity of about 10m/s, resulting in flight Reynolds numbers of $7x10^4$ to $2x10^5$. At this flight rynolds number range laminar separation bubble formed on the airfoil exhibits performance deterioration in terms of lower lift, higher drag and stall characteristics[1]. However the flow field on low aspect ratio wing planform (MAV) is highly three dimensional due the formation of vortical structures from the wing tip[2-3].This vertical structures minimizes the spanwise extent of laminar separation bubble on the low aspect wing. The tip vortex enhances the performance of MAV configuration in terms of higher lift (non-linear contribution) and stall angle compared to airfoil [4. Numerical and experimental stdudy of flow structure on low aspec ratio wing showed bilateral symmetry in vortical structures from the tip at angle incidence 10° and bilateal asymmetry at angle of incidence 35°[5]. Recently, PIV (2D and strereo) studies on micro air vehicle wing planform reported the formation

[1] Scientist, Experimental Aerodynamics Division,
[2] Graduate Trainee, Experimental Aerodynamics Division,
[3] Head, Experimental Aerodynamics Division, Associate Fellow AIAA.

of counter rotating vortical structures from the tip and laminar separation bubble in the reflexed region of the wing planform at the mid span[6]. It should be noted that, these studes excluded the the influence propeller induced flow on the aerodynamic characteristics and the associated flow field on low aspect ratio wing planform. In general, propeller covers nearly 50% of the span of MAV wing planform. It is expected that the interaction of the propeller slipstream with wing planform strongly influences the aerodynamic characteristics of the MAV. Efforts were made in the past to study the effect of propeller induced flow on the aerodynamic characteristics of MAV with pusher and tracter configuration. The results from these studies shown the enhancement of aerodynamic characteristics of the wing, increase lift and delay in stall in power on condition.This performance improvement is function of location and orientation and of propeller from the fuselage with respect to wing[7-10]. A recent study investigated the effect of propeller induced flow on aerodynamic characteristics of fixed wing MAV, through a decoupled motor and propeller arrangement for force measurements. This study showed significant increase in lift and stall angle under propeller-on condition[11] . Gamble and Reeder[12] carried out force measurements as well as a velocity field mapping using 3-component hotwire on rigid and flexible wing MAV under propeller-on condition. However a complete flow field mapping on MAV wing planform in the presence of a propeller slipstream has not yet been reported in the litereature.

The present work is to invstigate flow field qualitatively (oil flow) and quantitatively (Stereo Particle Image Velocimetry) on a low aspect ratio modified inverse Zimmerman planform under propeller-on and off conditions at low Reynolds number .The oil flow studies were carried out at several incidences to understand the evolution of flow field on MAV with and without presence of propeller slipstream. Propeller induced flow field on a low aspect ratio wing planforms at low Reynolds number will be helpful to understand the aerodynamics of fixed wing micro air vehicles (MAVs) and provide data base for validation of numerical and computational models results in design of better flight performance MAVs.

II. Experimental Details

Wind tunnel experiments were conducted in 1.5m x 1.5m (Fig 1) in-draft open circuit low speed wind tunnel at National Aerospace Laboratories. The tunnel has 12:1 contraction and 6.5m length test section. It has the capability to achieve the speed of 5-50m/s. Tunnel turbulence level in test section is 0.1% up to 40m/s and the mean velocity uniformity in the test section plane is within ±0.3%.

The Flow visualization and Stereo-PIV mesurements were carried out on typical fixed wing-MAV model(Fig.2).The model has a high wing configuration with modified inverse Zimmerman wing planform. The cross section of the wing is a Selig 4083 airfoil camber with maximum camber of 3% located at 40% from the leading edge. The wing planform has a root chord of 250mm and span of 300m with uniform thickness of 3mm. The aspect ratio of the wing planform is 1.46. The wing planform is attached with fuselage of rectangular configuration with a stub front end and a boat tail at the rear.

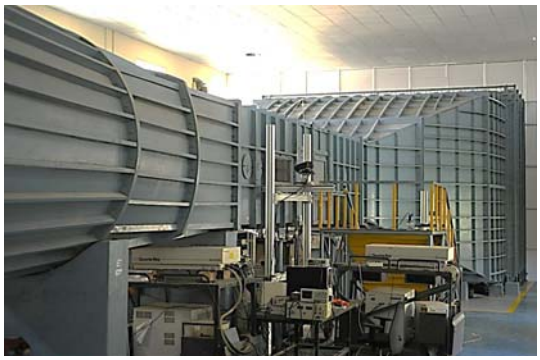

Fig.1 Photograph of the wing tunnel facility

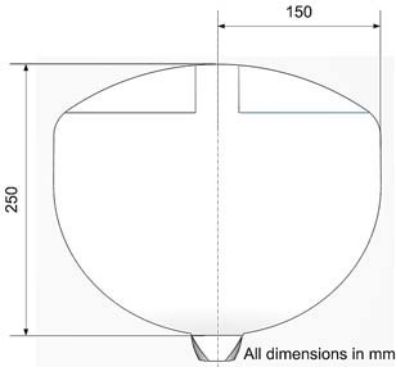

Fig.2 Schematic of the windtunnel model

The model was mounted in the wind tunnel through a sting supported by pitching sector mechanism(Fig.3). The tests were conducted at freestream velocity of 10m/s, corresponding to Reynolds number based on root chord of about 160000. Motor and propeller arrangement is mounted on the nose of fuselage for power-on measurement.The propeller is kept to run at constant rpm of 8500 for power-on measurements,which has produced a steady level flight for a flying model at zero angle of incidence at 10m/s[11]. The motor is AXi 2203/46 (KV 1720) DC brushless motor and the propeller is a GWS 7”x3.5” propeller. The motor was powered by an external DC power supply from

outside the tunnel. The propeller rpm is monitored in the oscilloscope outside the tunnel through TACHO meter (monted on the sting) output connected to the oscilloscope. The rpm of the propeller was controlled by setting the required voltage by monitoring propeller rpm in the oscilosecope.The variation in the propeller rpm due to voltage fluctuation and tunnel freestreamvelocity variation is ±50rpm. Motor and propeller has been removed from the fuselage for the measurement at power-off condition.

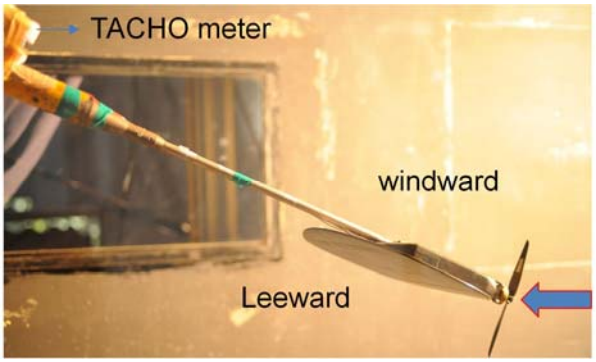

Fig.3 Photograph of the model mounted on the sting

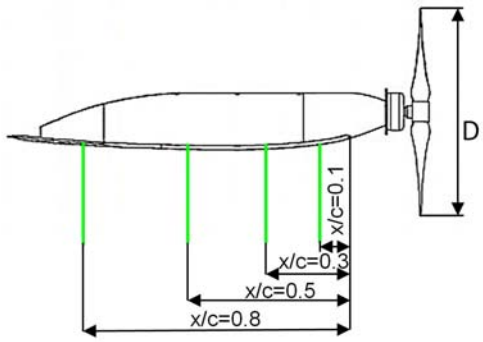

Fig.4 SPIV measurement planes

Qualitative (surface oil flow visualization) and quantitative (particle image Velocimetry) flow field measurements were made on the MAV model for both power-off and power-on condition. Surface flow visualization was carried out using the mixture of titanium dioxide, oleic acid and SAE 60 grade vacuum pump oil in the ratio of 1:5:7. The mixture was sprayed on to the model by means of repeated flicking of the bristles of a paint brush untill the model was covered with uniformly sized, discrete dots of a size that did not move under the influence of gravity. The tunnel flow was then brought on flow condition as rapidly as possible and the streamlines then formed naturally on the surface of the model due to surface flow shear. The tunnel was run until the oil had stopped flowing and with the tunnel off, the model was photographed. Oil flow visualization was carried out on MAV model at angle of incidence of 10º, 15º, 20º, 24º with propeller-on and off condition. The uncertainty in angle of incidence of the pitching sector mechanism is ±0.1°. The angles of incidence were selected from the previous force measurement studies on the same planform, shown significant difference in lift coefficient between propeller-on and off condition [11]. Stereo PIV measurements were done at four chord wise planes (fig.4) at angle of incidence of 24º where the oil flow visualization showed substantial difference in the flow pattern on the planform between propeller-on and off condition.

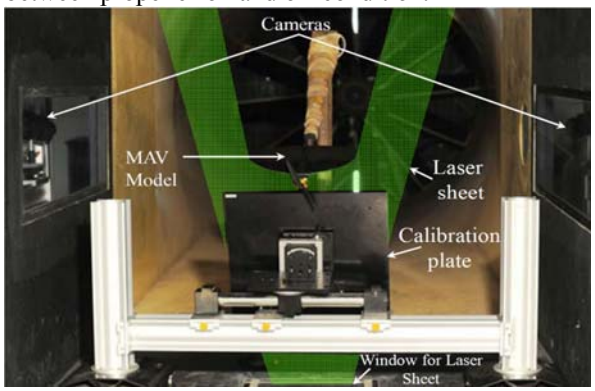

Fig.5a Photograph of the SPIV experimental setup

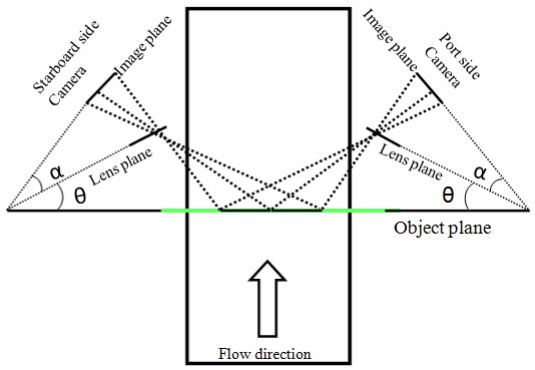

Fig.5b Schematic of the SPIV experimental setup

.Stereo-PIV images were acquires through MotionPro Y5 camera of 2314(H)X1728(V) pixels with Nikkor 85mm Schiempflug lens The photograph and schematic of the experimental setup for stereoscopic particle image celocimetry is shown in Fig 5a&5b .Two MotionPro Y5 cameras were mounted on either sides of the tunnel. The angle of image plane of the port and starboard side camera with respect to object plane is kept θ=44.75° and 45.5° respectively such a way that the axis of both the camera coincides at the center of the object plane. Sheimpflug condition (rotation of image plane with respect to lensplane(α) applied throgh the Sheimpflug mounts in the lense to

make the image plane, lense plane and object plane in collinear. This ensures the entire area in the object plane in good focus.

The flow-field with tracer particles is illuminated by a double pulsed, frequency doubled dual Nd:YAG, PIV 400 laser, providing with a nominal 400 mJ of energy per pulse at a 532-nm wavelength. The optimum performance of the laser is at 15Hz (15 pairs per second). The beam from the laser is spread as a thin sheet of light with nearly flat intensity profile in the measurement plane using a few optical components to achieve a sheet thickness of 1mm. This arrangement provided a flat imaging area of 200 mm x 400 mm at the planeson model.The camera and the light sheet were moved at equal distance to use the same calibration settings for the image processing at each planes. The synchronization of laser and the camera image acquisition was achieved through IDT motion-PRO timing hub. The post processing of the acquired images were carried out with IDT pro VISION software. Mean velocities were estimated from ansemble average of 2000 image pairs. The laser pulse separation time was kept at 7μs to allow the particle to move about one fourth of the sheet thickness for the maximum velocity in the measurement. The velocity vectors were estimated from processing image with 24X24 pixel interrogation window and 50% overlap. The spatial resolution with this setting is 5mm in both directions is achieved in the final dataset. The flow field was seeded by the injecting the fog of particle size 5μm in the wind tunnel entry section.

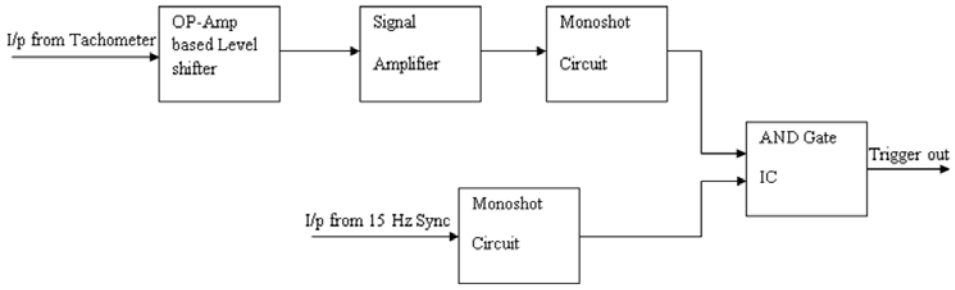

Figure 6 Block diagram of triggering circuit for laser

.

The fog was generated by the commercially available fog liguid (ehtlene glycol) through ANTARI Z3000 fog maching. The ability of the seeding particles to flow the over the model was ensured through evaluating the settling speed of the particle(U_s) under gravity($U_s = g(\rho_p - \rho_f)^2 d_p / 18\mu_f$), where g, ρ_p ,ρ_f ,d_p *and* μ_f are acceleration due to gravity, particle density, fluid density, particle diameter and visocity of fluid [13]. The settling speed for the particle(0.005m/s) used in the present measurement is negligible compared to the flow velocity(10m/s), which ensured the particle following the flow. The uncertainty analysis in stereo-PIV measurements based on the method of Zang and Prasad [14] indicates that the errors of the determined velocity vectors are about ±1.5% of the actual velocity components.

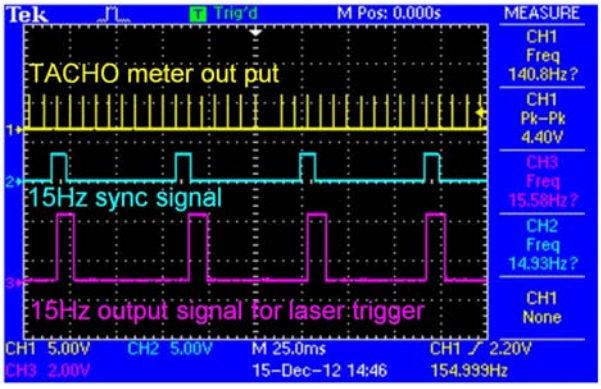

Fig.7 Screen shop of synchronization signal in osciloscope

To carry out phase averaged stereo PIV measurement behind a propeller blade at a position nomal to the chord of the wing planform, the passage of the propeller blade and the laser triggering needs to be synchronized. Since the propeller running frequency (140Hz at 8500rpm) and the laser triggering frequency (15Hz) are not same, a circuit has been made to get the 15Hz trigger output signal for laser which is synchronizesd with desired propleller position with respect to wing chord. The block diagram of the triggering circuit is shown in Fig.6. A TACHO meter was

mounted on the sting of the pitching sector mechanism to get the frequency signal of the propeller RPM. The TACHO gives 300mv ac on the 5v dc shift signal. The dc offset voltage has been cut off with the level shifter and 300mv ac was amplified. This amplified output has been given to mono shot to generate the digital pulses at 1.6 percent of duty cycle. Synchronized pulse of 15Hz given to another monoshot to generate the pulse of 10 percent of duty cycle. These pulses were given to ANDDING operation to generate the 15Hz trigger output signal of 12 percent duty cycle. This output signal has been given to timer box to trigger the lasser. The oscilloscope screen shot of output signals in this process is shown in Fig .7. the pulse separation time between the two laser beem is kept at 7µs. The agular displacement of propeller blade porsition between the pulse of 5µs in each pair is 0.25 °.

III.Results and Discussion

A. Flow visualization

Oil flow pattern on the wing planform at 10º, 15º,20º, 24º angles of incidence with propeller-on and off condition is shown in Figures 8-11.It has been clearly seen from the oil flow patern, the primary attachment line moves towards the inboard of the wing planform with increase in the angle of incidence. At angles of incidence 10° and 15°, the flow pattern does not shown any difference on the location of primary attachment as well as secondary separation, and the extent of primary vortex region between propeller-on and off condition. However, when the propeller is on, the secondary separation location moved towards leading edge in the inboard region near fuselage.

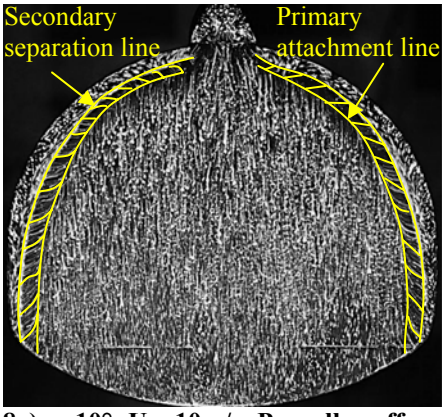

8a) α=10°; U_∞=10m/s; Propeller-off

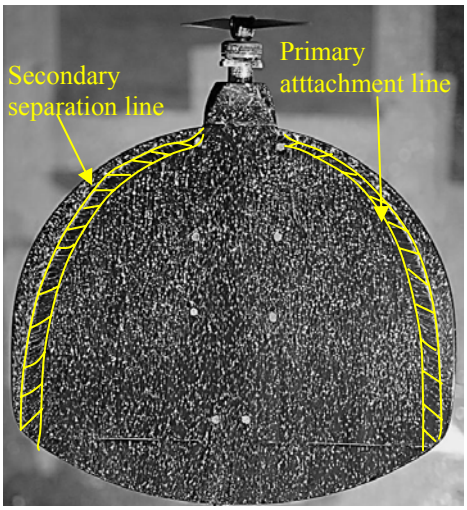

8b) α=10°; U_∞=10m/s; Propeller-on

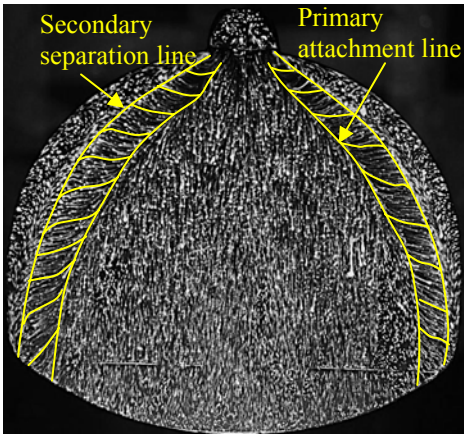

9a) α=15°; U_∞=10m/s; Propeller-off

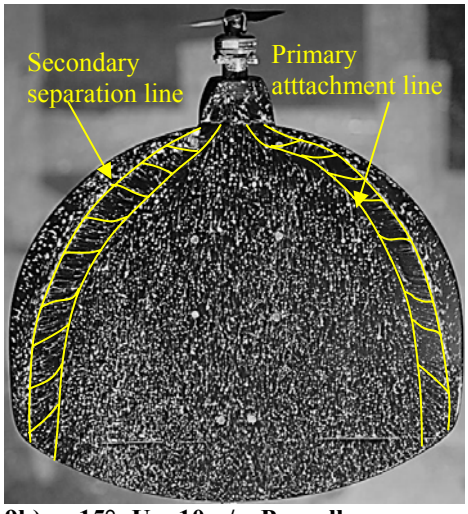

9b) α=15°; U_∞=10m/s; Propeller-on

At 20º the vortex moved inboard and grown in size compare to that of angle of incidence 10º and 15º for the propeller-off condition. When the propeller is on, in contrast to the incidence of 10º and 15º , here the asymmetry of vortices becomes pronounced. However, the tendency of the secondary separation line to move towards the leading edge remains. At 24º the vortical flow is pushed inboard and is dissipated on the port side for the propeller-off condition. As seen from fig.11b switching on the propeller results in attached flow on port side as well as small asymmetry prevails on the planform.

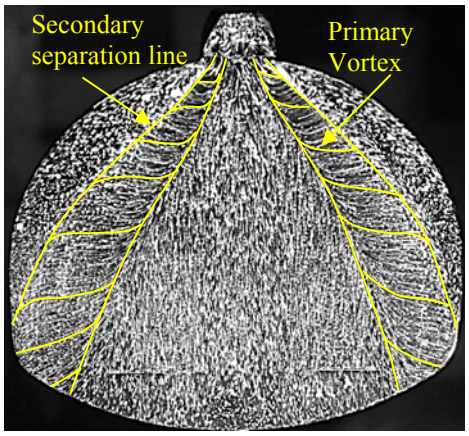

10a) α=20°; U∞=10m/s; Propeller-off

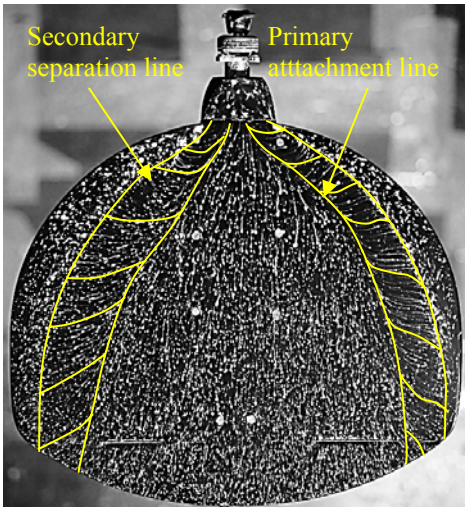

10b) α=20°; U∞=10m/s; Propeller-on

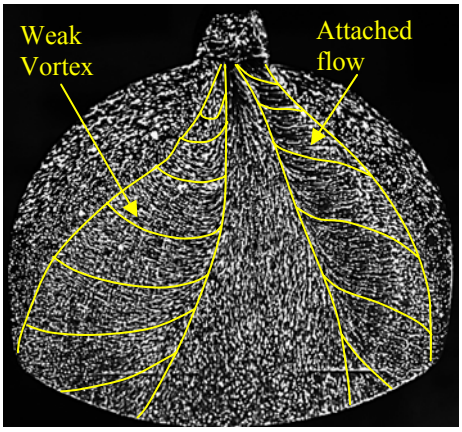

11a) α=24°; U∞=10m/s; Propeller-off

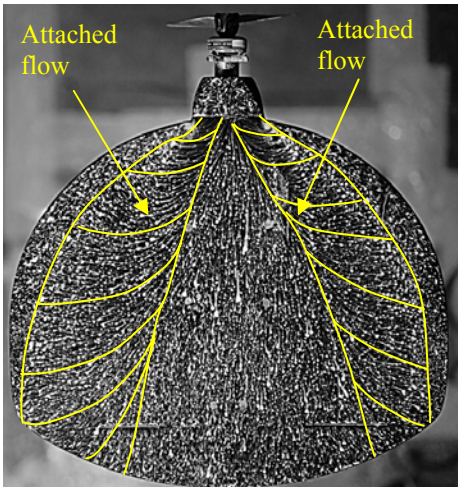

11b) α=24°; U∞=10m/s; Propeller-on

B. Stereo PIV measurement

Stereo PIV measurements were carried out at four planes along the chord (x/c=0.1, 0.3,0.5&0.8) on the planform for propeller-on and off condition at angle of incidence 24º. Mean streamwise velocity contour at all measurement planes is shown in Fig 12a&12b for propeller-on and off condition respectively.when the propeller is off, the streamwise velocity contour has shown negative velocity region with small magnitude close to the surface of the planform. This low velocity region grows in size from leading edge to trailing edge. It has been seen that the the countour level in the low velocity region changes from neagative to positive or zero contour levels as it grows towards trailing edge. This is similar to the wake like axial velocity profile generally seen on low sweep non-slender delta wing at high angle of incidence in low Reynolds number. This wake like velocity profile usually observed in the post vortex breakdown angle of incidence on the low sweep non slendler delta wing. However this nature of flow is confined within in the vortex core[15-16]. In the propeller on case, the propeller slipstream

increases the magnitude of streamwise velocity behind the propeller in all the measurement planes and a significant reduction of magnitude and region of negative streamwise velocity (reverse flow) is seen near the planform surface.

Figure 13a and 13b shows the contour of vertical velocity component at four measurement planes for propeller on and off condition. The negative and positive magnitude in vertical velocity contour clearly shows its contribution to bring the flow towards the planform surface and lift the flow from the surface respectively.. The magnitude of the

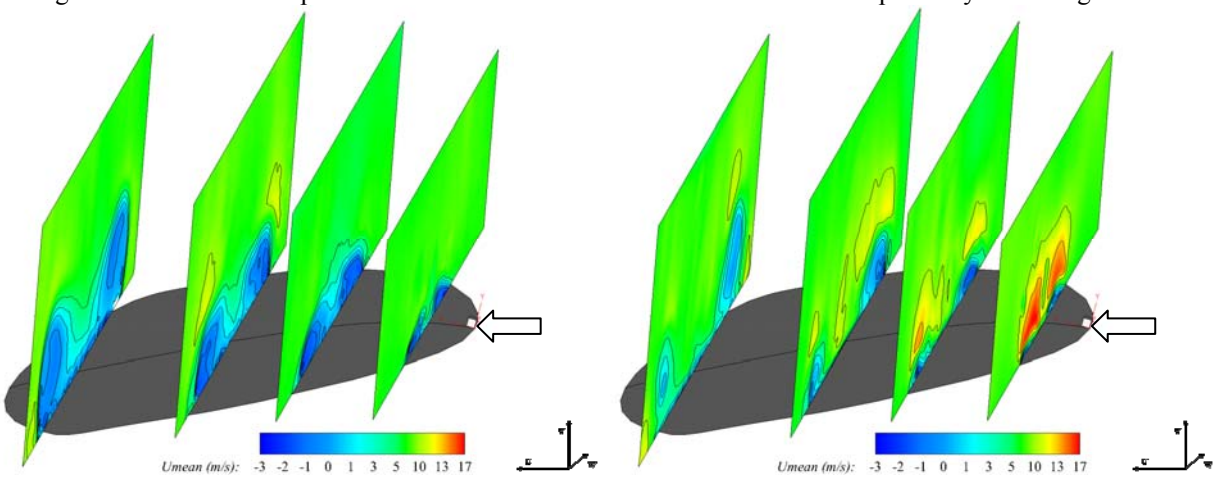

a) propeller-off condition **b) propeller-on condition**

12.Mean streamwise velocity contour at α=24°

positive vertical velocity has higher value in the port side compared to starboard side for the propeller off condition. At x/c=0.5and 0.8, the magnitude of negative vertical velocity was increased and it is distributed almost equal level, except away from the port side tip. This difference in positive and negative vertical velocity contour between port and starboard side clearly correlates the asymmetry seen in oil flow patern. For the propeller on condition, the magnitude and region of negative vertical velocity is increase and its distributed equally about mid span. The magnitude of negative vertical velocity is almost equal to the positive values on the planform. There is an increase in magnitude of positive values of vertical velocity away from port side tip of the planform due to the propeller rotation in the same direction.

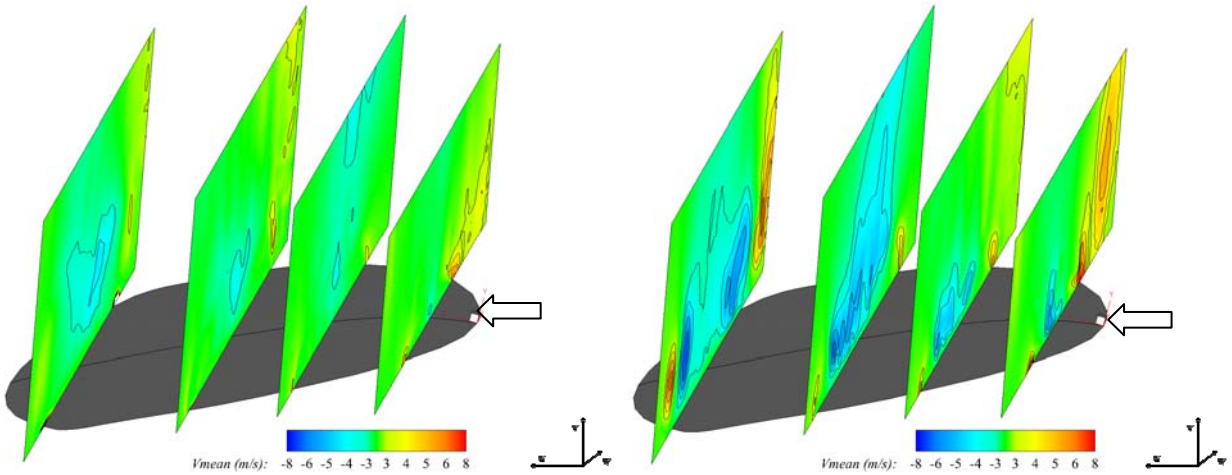

a) propeller-off condition **b) propeller-on condition**

13.Mean vertical velocity contour at α=24°

The tangential velocity contour for the propeller off condition clearly shows(Fig.14a) that the magnitude of tangential velocity is lower in the portde side of the wing planform compared to the starboard side at x/c=0.1and 0.3. At downstream distances x/c=0.5 and 0.8, the magnitude increases on both sides and it becomes nearly equal. In propeller on condition (Fig.14b), it has been seen that the tangential velocity contour is almost symmetry and its magnitude increases from leading edge to trailing edge similar to propeller off condition.

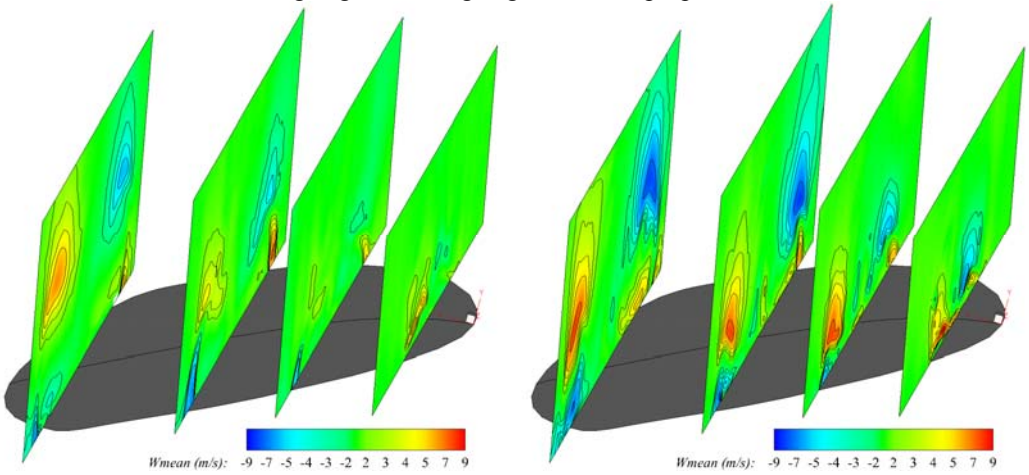

a) propeller-off condition **b) propeller-on condition**

14.Mean tangential velocity contour at α=24°

The magnitude of vertical and tangential component causes the flow to move towards the surface of the planform and flow becomes attached on to the surface. In propeller off condition, both negative magnitude of vertical component and positive component of tangential component were lower in the port side compared to strarboard side at x/c=0.1 and 0.3. Due to this, separated/ weak vortex flow region is observed in the oil flow visualizations at these locations. Whereas in propeller on condition, both components were equal in magnitude on both sides, which was also seen in the attached flow pattern from the oil flow visualization.

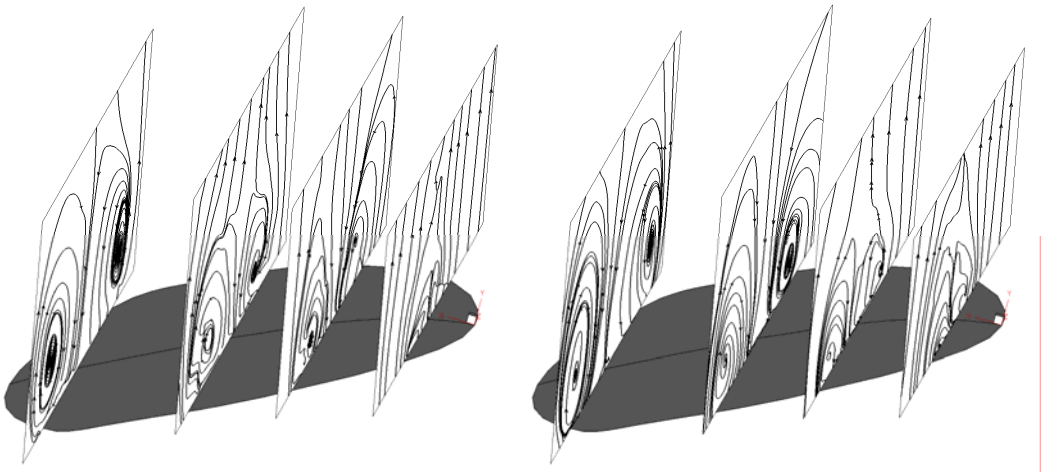

a) propeller-off condition **b) propeller-on condition**

15.Streamtraces of velocity field at α=24°

Stream traces at the four measurement planes for the propeller-on and off condition is shown in fig.15a and 15b. Streamtraces at x/c=0.1 shown elongated patern instead of well defined swirl pattern at the propeller of condition. Stream traces on the port the starboard side at x/c=0.3,0.5,0.8 reveals the clear swirl nature of the flow in the

starboard side with its centre close to the planform surface. However the corresponding planes at the port side has swirl flow center lifted away from the surface with elonganted stream straces in the plane at the x/c=0.2 . Previous study on vortex flow over low sweep delta wing at angle of incidence of 20° has shown the absence of swirl nature of flow in the apex region of the wing and re-establishment of swirl flow towards the trailing edge, suggesting that the breakdown of the vortex in the apex region and restoring the vortex in the downstream region[17]. The similar flow patern is observed in the persent study. The lifting up of the vortex flow field in the port side is the cause for the asymmetry in the oilflow patern at angle of incidence 24°. The stream traces showed the center of the swirl moved near wing surface at all the measurement planes in the propeller on condition, which explains the well attached flow in the port side seen in the oil flow pattern in propeller on condition.

IV. Conclusion

Propeller induced flow on a typical micro air vehicle was investigated through surface oil flow visualization and strerioscopic particle image velocimetry at low Reynolds number. Comparison of surface flow topology and off surface velocity field on the MAV planform were made between propeller-on and off conditions. At medium angles of incidence (10º and 15º), there is no much change in the flow field seen in the oil flow pattern. At higher angles, significant changes in flow pattern were observed. At 20 ºangle of incidence, the propeller slipstream makes the vortex to move significantly outboard and flow becomes mildly asymmetry. At 24º angle of incidence for propeller-off condition, the port side vortex is highly weekend and is pushed outboard pronounced asymmetry in the flow topology. The propeller-on case at this angle results in restoration of attached flow in the portside and moves both vortices outboard especially near the leading edge.The stereo PIV measurements results carried out at 24º incidence correlate well with the oil flow patterns. The asymmetry in the flow field is observed similar to the oil flow pattern at 24º incidence in propeller off condition. The streamwise velocity component increases throughout the planform by the propeller slipstream. The increase in the magnitude of tangential and vertical velocity component by the propeller slipstream brings the swirl flow close to the wing surface on the portside and made the attaché flow in portside seen in the oil flow pattern. The results yield an insight into the significant modification of flow over the MAV wing due to the propeller . This study has brought out the importance of the propeller inuced to be considerd for the design and optimaization wing planform for the for better aerodynamic performance.

Acknowledgments

The authors would like to acknowledge the efforts of the technical staff Mr.Nitin Prakash Pawar, Mr.Varadharaj and Mr.Khem singh in carrying out the experiments in the 1.5m Large Low Speed Wind tunnel. The technical support of Mr.Ramachandra during the model fabrication is gratefully acknowledged.

References

[1] Mueller, T.J. and Delaurier J.D “Aerodynamics of small vehicles”, *Annual Review of Fluid Mechanics*, Vol.35, 2003, pp 89-111

[2] Torres, G.E and Mueller, T.J “Low-Aspect-RatioWing Aerodynamics at Low Reynolds Numbers”, *AIAA Journal* Vol.42, No.5, 2004, pp.865-873

[3] Pelletier,A.,and Mueller,T.J “Low Reynolds Numbers Aerodynamics of Low-Aspect-Ratio tThin/Flat/Cambered-Plate Wings”, *Journal of Aircraft*, Vol.37, No.5, 2000, pp.825-832

[4] Shyy, W. Aerodynamics of Low Reynolds Number Flyers. Cambridge: *Cambridge University Press*, 2008

[5] Jian, T. A. N. G., and Zhu Ke-Qin. "Numerical and experimental study of flow structure of low-aspect-ratio wing." *Journal of Aircraft* 41.5 (2004): 1196-1201.

[6] Parvez Khabatta, Lawrence Ukeiley, Charles Tinney, Bret Standford and Peter Ifju, “ Flow Characteristics of a Three-Dimensional Fixed Micro Air Vehicle Wing’, *AIAA*, 2008-3020

[7] Thipyopas, C. and Moschetta, J., "Comparison Plusher and Tractor Propulsion for Micro Air Vehicle Applications," *SAE Technical Paper* 2006-01-2397, 2006

[8] Null, W., Noseck, A., and Shkarayev, S., “Effects of Propulsive-Induced Flow on the Aerodynamics of Micro Air Vehicles”, *23rd AIAA Applied Aerodynamic Conference*, 2005-4616

[9] Catalano, F.M., “On the Effects of an Installed Propeller Slipstream on Wing Aerodynamic Characteristics”, *Acta Polytechnica*, Vol.44 ,No.3, 2004.

[10] Choi, Sungjin, and Jon Ahn. "A Computational Study on the Aerodynamic Influence of a Pusher Propeller on a MAV." *40th Fluid Dynamic Conference and Exhibit*. Vol. 28. 2010.

[11] Arivoli.D, Ravi Dodamani, Roshan Antony, Suraj.C.S, Ramesh.G, and Sajeer Ahmed, “Experimental Studies on a Propelled Micro Air Vehicle”, *29th AIAA Applied Aerodynamics Conference*, 2011

[12] Gamble, B., and Reeder, M., "Experimental Analysis of Propeller-Wing Interactions for a Micro Air Vehicle", *Journal of Aircraft*, Vol.46, No.1, January-February 2009
[13] Prasad, Ajay K. "Particle image velocimetry." CURRENT SCIENCE-BANGALORE- 79.1 (2000): 51-60.
[14] Zang, Weijun, and Ajay K. Prasad. "Performance evaluation of a Scheimpflug stereocamera for particle image velocimetry." Applied optics 36.33 (1997): 8738-8744.
[15] Ol, M. V. and Gharib, M., "Leading-Edge Vortex Structure of Nonslender Delta Wings at Low Reynolds Number," *AIAA Journal* Vol. 41, No. 1, January 2003, pp. 16-26
[16] Rullan, Jose M. The Aerodynamics of Low Sweep Delta Wings. Diss. Virginia Polytechnic Institute and State University, 2008.
[17] Taylor, G. S., Schnorbus, T., and Gursul, I., "An Investigation of Vortex Flows over Low Sweep Delta Wings," *AIAA Fluid Dynamics Conference*, Paper No. AIAA-2003-4021, Orlando, FL, June 23-26, 2003.